Numerical Investigation of Laminar Flow Heat Transfer Through Helically Coiled Tubes Using Al_2O_3 Nanofluid

Ahmed M. Elsayed[1], Raya K. AL-Dadah[1,*], Saad Mahmoud[1], Abdel-Fattah Mahrous[1]

* Corresponding author: Tel.: +44 (0)121 414 3513; Fax: +44 (0)121 414 3958; Email: R.K.Al-dadah@bham.ac.uk

1: School of Mechanical Engineering, University of Birmingham, B15 2TT, UK.

Abstract Nanofluids have been reported to enhance heat transfer performance in heat exchangers. Additionally, the use of helical coils has shown to be another passive heat transfer enhancement technique. This work presents a CFD modeling study to investigate the laminar heat transfer through helical tubes with nanofluids. The developed CFD models were validated against published experimental results and empirical correlations in the literature. The effects of particles concentration and Reynolds number on heat transfer coefficient were numerically investigated. Results have shown that Al_2O_3 dispersed in water increases the heat transfer coefficient in helical coils by up to 4.5 times that of pure water in straight tubes at same Reynolds number. For concentrations larger than 2%, Al_2O_3 is more suitable for thermal systems of small thermal loads where the pumping power is not critical.

Keywords: Nanofluids, Helical coils, CFD, Fluent.

1. Introduction

Since the fuel crisis in the seventies, heat transfer enhancement techniques have received significant attention. Active, passive and compound heat transfer enhancement methods have been developed. Passive methods were preferred due to their simplicity in manufacturing, lower cost and longer operating life. Helical coils, additives to fluids, swirl flow devices, rough and extended surfaces are all passive enhancement techniques (Bergles, 2002). Helical coils have been shown to be effective in enhancing single phase heat transfer (Kumar et al., 2006), boiling heat transfer (Wongwises and Polsongkram, 2006 ; Elsayed et al., 2010) and condensation heat transfer (Wongwises and Polsongkram, 2006b; Shao et al., 2007).

Nanoparticles improve the energy transport properties of the base fluid by increasing the effective thermal conductivity and heat capacity, which enhances the heat transfer rate of the nanofluid. The chaotic movement of ultra fine particles accelerates the thermal dispersion process in the fluid which leads to a steeper temperature gradient between the fluid and the wall augmenting

heat transfer rate (Li and Xuan, 2002). The applications using these Nanofluids include engine cooling to reduce the engine weight and fuel consumption (Saripella et al., 2007), increasing the critical heat flux in boilers (Cheng, 2009) and developing compact heat exchangers for medical applications (Sundar et al., 2007).

Recently, many researchers have experimentally investigated the effect of nanofluids in enhancing the heat transfer coefficient in straight tubes such as (Heris et al., 2006) using alumina (Al_2O_3), copper oxide (CuO) and copper (Cu) nanoparticles dispersed in water, (Murshed et al., 2007) using titanium dioxide (TiO_2) dispersed in water, and (Rea et al., 2009) using Al_2O_3 and zirconia in the laminar flow regime.

Experimental data of Heat transfer and pressure drop using nanofluids in helical coils are very limited. Wallace (2010) measured the heat transfer rate using nanofluids in helically coiled cooler however the author did not report any measurements of heat transfer coefficients or wall temperatures. Akhavan-Behabadi and Hashemi (2010) tested the pressure drop using CuO dispersed in oil flow in a helical coil but no heat transfer measurements were carried-

out. With the lack of experimental data, the CFD prediction of single phase heat transfer becomes a useful tool to investigate the performance of nanofluids in helical coils. This work investigates the effect of particle concentration and Reynolds number on the thermal performance of Al_2O_3 nanofluid in helically coiled tubes in the laminar flow regime.

2. Flow governing equations and thermophysical properties

Al_2O_3 nanofluid has been treated as incompressible, steady state, homgenuous and Newtonian fluid with negligible effect of viscous heating. The flow has been modelled using Navier-stokes equations using fluent package. The single phase homogeneous flow governing equations in the Cartesian co-ordinates are:

Continuity: $\rho \nabla \bullet \vec{V} = 0$ (1)

Momentum: $\rho \ (\vec{V} \bullet \nabla) \ \vec{V} = -\nabla P + \rho \vec{g} + \mu \nabla^2 \vec{V}$ (2)

Energy: $\rho C \ (\vec{V} \bullet \nabla) \ T = k \nabla^2 T$ (3)

The effective thermo-physical properties of the nanofluid were defined as (Rea et al., 2009):

Density:
$$\rho_{nf} = (1-\phi)\rho_{bf} + \rho_p \phi \qquad (4)$$

Specific heat:
$$C_{nf} = ((\rho C)_p \phi + (\rho C)_{bf}(1-\phi))/\rho_{nf} \qquad (5)$$

Thermal Conductivity:
$$k_{nf} = (1+4.5503\phi)k_{bf} \qquad (6)$$

Dynamic viscosity:
$$\mu_{nf} = \exp(4.91\phi/(0.2092-\phi))\mu_{bf} \qquad (7)$$

Where *nf, bf* and *P* denote the nanofluid, base fluid, and particle respectively. The base fluid thermo-physical properties have been fitted as polynomial functions in temperature (Kelvins) using Engineering Equation Solver EES data as shown in equations 8 to 10.

$$\rho_{bf} = 2813.77E(-01) + 6351.93E(-03)T \qquad (8)$$
$$- 1761.03E(-05)T^2 + 1460.96E(-08)T^3$$

$$k_{bf} = -1056.42E(-03) + 1011.33E(-05)T \qquad (9)$$
$$- 1772.74E(-08)T^2 + 7994.88E(-12)T^3$$

$$\mu_{bf} = 9684.22E(-05) - 821.53E(-06)T \qquad (10)$$
$$+ 2345.21E(-09)T^2 - 2244.12E(-12)T^3$$

These properties were formulated as UDF subroutine and incorporated into Fluent 6.3 solver.

3. Heat Transfer in Straight Tubes

3.1 Base fluids (water) heat transfer in straight tubes

The CFD analysis for the base fluid flow in straight tube was investigated to provide a reference case. Fig.1-a. shows the boundary conditions and mesh configuration for a straight tube with 4.5mm internal diameter and 1.01m long. The fluid enters at uniform velocity at the tube inlet and the tube wall exposed to uniform heat flux. The flow in the straight circular pipe is a three-dimensional problem in Cartesian coordinates which reduced to a two-dimensional analysis via symmetry in cylindrical polar coordinates.

Enhanced mesh treatment was applied at inlet and wall boundaries with 50 x 700 nodes in the radial and axial directions respectively with successive ratio of grid in the radial direction of 1.1. Second order upwind scheme was utilized for discretizing the energy and momentum equations, and the SIMPLE algorithm was used for solving the pressure-velocity coupling.

The average heat transfer coefficient was calculated as the arithmetic mean of the locally predicted heat transfer coefficients. Fig. 1-b shows the predicted heat transfer coefficient and those reported by (Rea et al., 2009) at various Reynolds numbers with ±7% agreement.
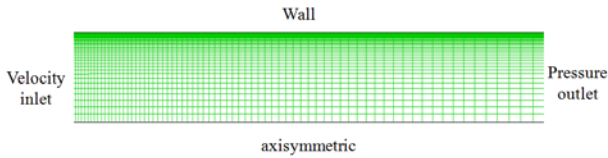
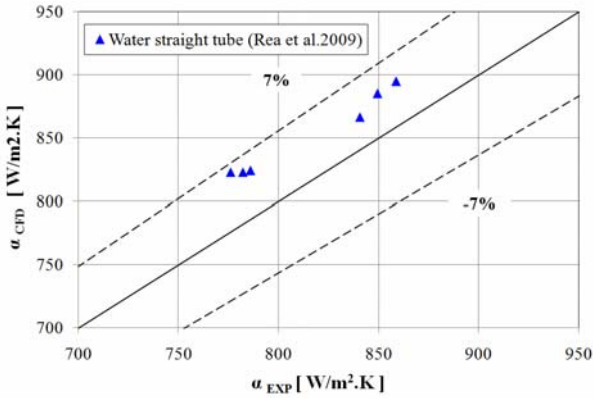Fig. 1-a Meshing of the straight tube.

Fig. 1-b. Validation of water (base fluid) CFD model in straight tubes.

3.2 Al₂O₃ nanofluid heat transfer and pressure drop analysis in straight tubes.

The flow governing equations describing nanofluids flow (Equations 1 to 10) were used to simulate the Al₂O₃ nanofluid performance in straight tube. Fig. 2 presents the predicted heat transfer coefficient of Al₂O₃ nanofluid in straight tube compared to the experimental results of Rea et al., 2009 at volume concentration ratios of 0.65%, 1.32%, 2.76% and 6% and Reynolds numbers ranging from 400 to1800 with ±10% agreement.
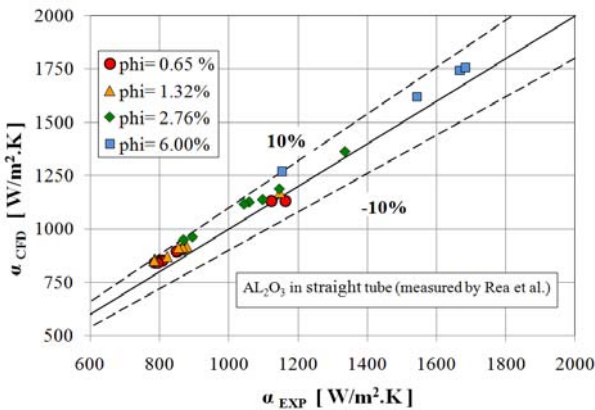

Fig. 2. Validation of Al₂O₃ nanofluid CFD model in straight tubes.

The developed CFD model has been used to investigate the effect of nanofluid volume fraction on the heat transfer enhancement ratio in straight tubes at various Reynolds Numbers. In this analysis, the heat transfer enhancement ratio is defined as the ratio of heat transfer coefficient of the nanofluid to that of the base fluid at the same Reynolds number. Fig. 3 shows that the heat transfer enhancement ratio increases with the increase in nanofluid volume fraction and the increase in Reynolds number. However, for all concentrations used, the increase in heat transfer enhancement ratio is more noticeable at low Reynolds numbers (Re<1000). An enhancement ratio up to 1.55 (55%) was predicted at volume fraction of 4% and Reynolds number of 2000.

Analytical prediction of the enhancement ratio for the same tube diameter, tube length, and flow Reynolds number for developing laminar flow was deduced based on (Rea et al 2009) analysis for heat transfer coefficient at constant heat flux as shown in equations 11 and 12.

$$\alpha = fn\left(k^2 \rho V C / x d_i\right)^{1/3} \qquad (11)$$

$$Enhancement\ Ratio\ = \frac{\alpha_{nf}}{\alpha_{bf}} = \left(\frac{\left(k^2 \mu C\right)_{nf}}{\left(k^2 \mu C\right)_{bf}}\right)^{1/3} \qquad (12)$$

Where x, d_i, V, α are the local distance from entrance, internal tube diameter, flow velocity and heat transfer coefficient respectively. Results from the analytical prediction and the CFD were in agreement as shown in Fig. 3.
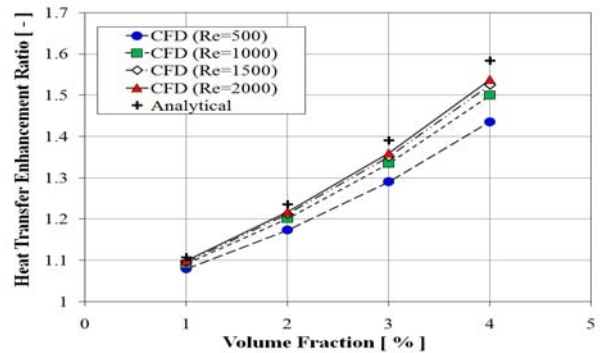

Fig. 3. Straight tube Al₂O₃ nanofluid heat transfer enhancement ratio at different Reynolds Number (q=5000 W/m²).

It has been shown that the friction factor of nanofluids agree with conventional theory (Li and Xuan, 2002). Therefore the ratio of pressure drop for nanofluid and base fluid in straight tube for constant tube length, tube diameter and Reynolds number is expressed as:

$$\frac{\Delta p_{nf,ST}}{\Delta p_{bf,ST}} = \frac{(\mu^2/\rho)_{nf}}{(\mu^2/\rho)_{bf}} \qquad (13)$$

Where Δp is defined as:

$$\Delta p = \frac{fL}{d_i}\frac{G^2}{2\rho} = \frac{fL}{d_i^3}\frac{\mu^2}{2\rho}\text{Re}^2 \qquad (14)$$

Fig. 4 shows the pressure drop ratio for the same Reynolds numbers and volume concentrations as those used in Fig. 3, where close agreement shown between the CFD and the analytical predictions.
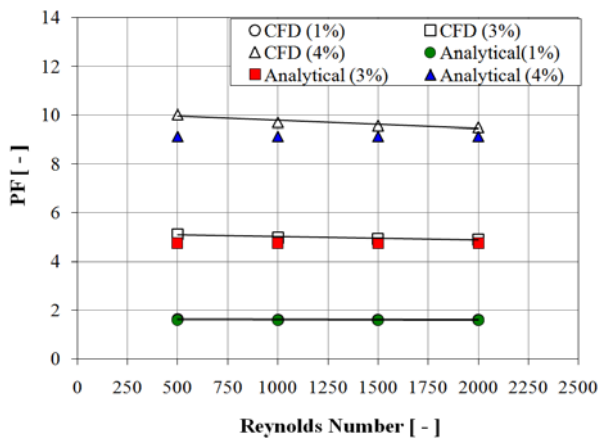

Fig. 4. Pressure drop Penalty factor in straight tubes.

4.0 Heat Transfer in Helical Coils

4.1 Base fluid (water) heat transfer in helical tubes

A helical coil with coil length and tube diameter similar to those used in the straight tube (Coil-A: 4.5 mm internal diameter and 1.01 m long) has been modelled. The coil pitch was selected as 15 mm and number of turns of 4 leading to a coil diameter of 80.373 mm. Fig. 5 shows the mesh used where Tri-quad meshing has been utilized to mesh the inlet face and hex/wedge cooper mesh used to mesh

the coil volume with 10 layers close to wall with growth factor of the grid in the radial direction of 1.3 and first layer thickness of 0.01 mm. The discritization schemes utilized were second order for energy, first order momentum, SIMPLEC algorithm with skewness factor of one for coupling the velocity and pressure.

A grid sensitivity analysis was carried out to determine the appropriate mesh density (number of cells per unit volume (cells/mm³)). Table 1 compares the simulation results of four grid densities of 14.28, 22.60, 31.74, 52.37, 63.86 cells per mm³. Grid densities larger than 60 nodes do not improve the prediction significantly in terms of average Nusselt number and wall temperature. As a result 60 nodes in the angular direction were utilized in the analysis with 5 hours simulation time required for each test condition.
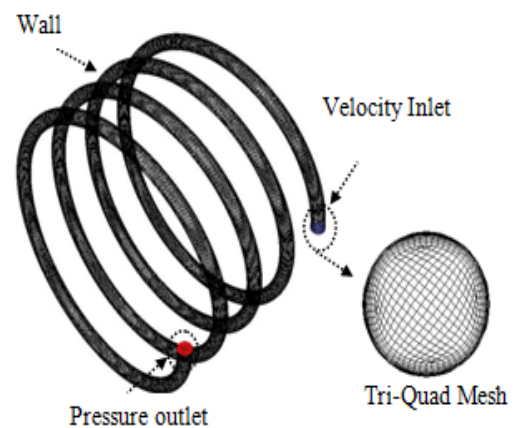

Fig. 5. Three dimensional mesh of helical coil using tri-quad mesh.

Table 1
Grid dependency analysis at water velocity=0.1 m/s and inlet temperature 20 °C.

Nodes in ang. direct.	20	30	40	60	70
Cell density cell/mm3	14.28	22.60	31.74	52.37	63.86
No. of Cells*1000	227.7	360.27	506	834.9	1018.1
ΔP (pa)	219.1	225.1	227.3	229.3	229.98
Avg.wall temp. (K)	301.21	301.35	301.44	301.55	301.52
Avg. Nusselt Number	16.17	14.85	13.95	13.17	13.15

Fig. 6 shows the effect of the number of nodes in the angular direction on the CFD results of Nusselt number at various water velocity and temperatures corresponding to various

Reynolds numbers and fluid properties. It can be seen that the Nusselt number becomes constant at 60 nodes in the angular direction corresponding to cell density of 52.37 cells/mm^3.
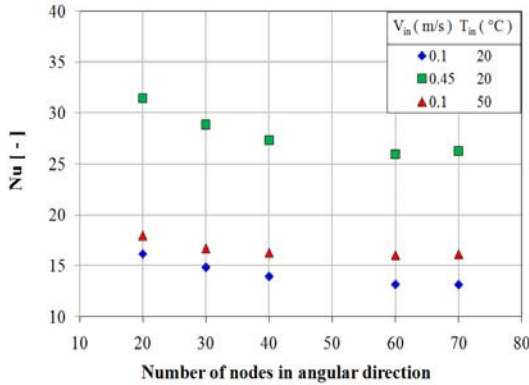

Fig. 6. Effect of cell density on the CFD results.

Fig. 7 shows close agreement between the CFD predicted heat transfer coefficient and those predicted using Manlapaz and Churchill (Rohsenow et al., 1998) and Kalb and Seader (1972) correlations given in equations 15 and 16. Manlapaz and Churchill validated their correlation for water, air and other fluids in helical coils exposed to constant heat flux with Reynolds numbers in the laminar flow regime. They correlated the Nusselt number as a function of Dean and Prandtl numbers in the following form:

$$Nu = \left[\left(4.364 + \frac{4.636}{x_3}\right)^3 + 1.816 * \left(\frac{Dn}{x4}\right)^{(3/2)}\right]^{(1/3)} \quad (15)$$

$$x_3 = \left(1 + \frac{1342}{Dn^2 \Pr}\right)^2 \qquad x_4 = \left(1 + \frac{1.15}{\Pr}\right)$$

$$Dn = \mathrm{Re}\left(\frac{di}{d_{coil}}\right) \qquad 0.1 \le \Pr \le 1600$$

Also Kalb and Seader numerically developed the following correlation (1972):

$$Nu_c = 0.913 Dn^{0.476} \Pr^{0.2} \qquad (16)$$

$$80 \le Dn \le 1200 \qquad 0.7 \le \Pr \le 5$$

The mean absolute relative deviation between the CFD prediction and empirical correlations was found to be less than ±3%.
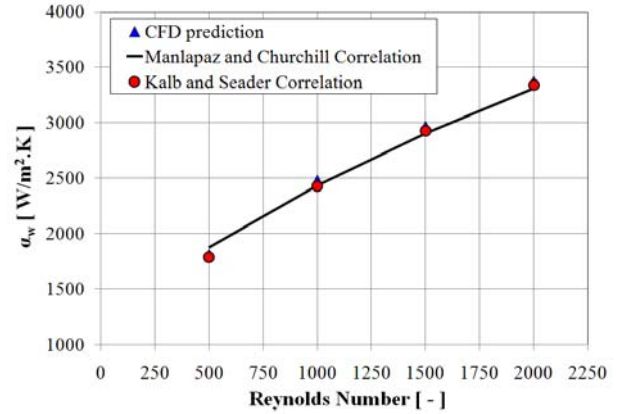

Fig. 7. Validation of CFD against empirical correlations for water flow in helical coils (q=5000 W/m^2).

Fig. 8 shows velocity contours at successive cross section in a plane parallel to the coil inlet. The flow enters the coil with uniform velocity of 0.11 m/s (Re=500) then the fluid elements with high velocities are pushed to the outer side of the coil due to centripetal force. This will generate a secondary flow with symmetric double vortices.
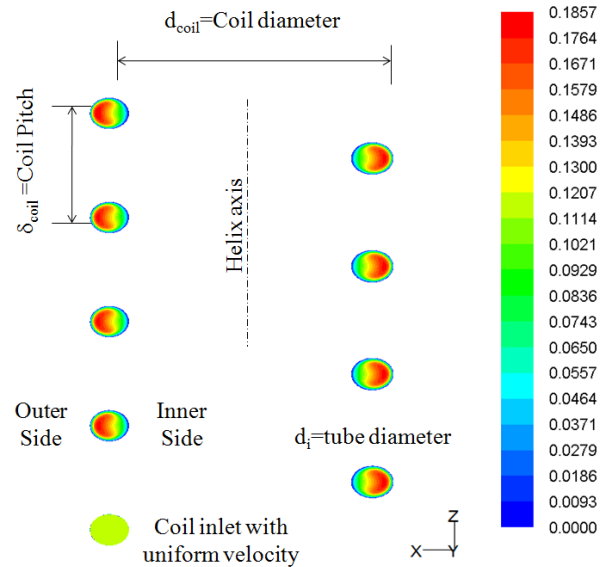

Fig. 8. Velocity contours with cross section parallel to coil inlet.

Fig. 9 shows the heat transfer coefficient distribution on the circumference of the tube at cross section of 3.5 turns from the coil entrance with flow velocity of 0.11 m/s. The heat transfer coefficient was found to be

lowest at the coil inner surface (position 1) where the wall temperature is highest compared to other positions in the section. The heat transfer coefficient at the bottom of the tube is slightly lower than that at the top due to the effect of gravity.
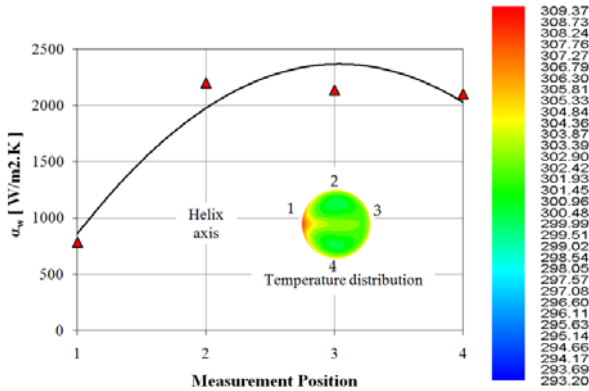

Fig. 9. Water heat transfer coefficient distribution on the circumference of the coil at 3.5 turns from entrance.

Fig. 10 shows the heat transfer enhancement ratio versus Reynolds number. The enhancement ratio is defined as the heat transfer coefficient of base fluid in helical coils compared to that of water flow inside straight tube with the same surface area. Three coils have been modeled with geometric characteristics shown in Table 2.

Table 2
Dimensions of helically coiled tubes in [mm]

Coil Number	d_i	d_{coil}	N_{turn}	δ_{coil}
Coil A	4.5	80.373	4	15
Coil B	4.5	40.1866	8	15
Coil C	6	80.373	3	15

Coil A shows that heat transfer enhancement ratios of 2.5 to 3.25 times that in straight tube was achieved. Fig. 9 shows that decreasing the coil diameter increases the heat transfer enhancement ratio due to better mixing caused by the larger number of turns. Increasing the coil tube diameter reduces the heat transfer enhancement ratio due to reduction in the flow velocity for the same Reynolds number.
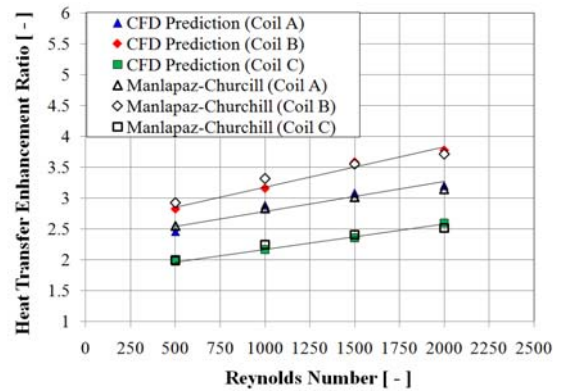

Fig. 10. Heat transfer enhancement ratio in helical coils using water at different Reynolds Number with different coils.

Comparing Fig. 10 to Fig. 3 indicates that the heat transfer enhancement ratio of helical coils (2-3.5) is higher than that of straight tube using Al_2O_3 nanofluids (1.55).

4.2. Al_2O_3 nanofluids heat transfer in helical coils

The flow governing equations describing nanofluids flow (Equations 1 to 10) and the geometry described in section 4.1 (Coil A) were used to simulate the Al_2O_3 nanofluid thermal performance in helical coil. With similar mesh configurations and boundary conditions, Fig. 11 shows the heat transfer enhancement ratio (heat transfer coefficient of nanofluid in the helical coil divided by the heat transfer coefficient of the base fluid in the straight tube with the same internal diameter and length) versus the nanofluid volume fraction at various Reynolds numbers. Contrary to the straight tube results, it is clear from this figure that as Reynolds number increases, the heat transfer enhancement ratio increases at all volume fractions.

The heat transfer using both nanofluids and helical coil effect was found to be very effective. An enhancement ratio was found to vary from 2.5 to 4.5 times that of base fluid (water) in straight tubes at Reynolds number of 500 to 2000 respectively. The combined enhancement technique found to be better than using helical coils with base fluids or using nanofluids in straight tubes.
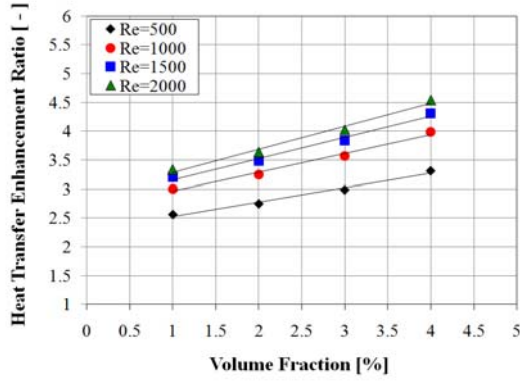
Fig.11. Heat transfer enhancement ratio in helical coil using Al_2o_3 nanofluid at different Reynolds Number (Coil A).

For the same tube length and Reynolds number, the pressure drop ratio of nanofluid flow in helical coil to the base fluid in straight tube can be expressed as:

$$\frac{\Delta p_{nf,Hc}}{\Delta p_{bf,St}} = \frac{f_{nf,Hc}}{f_{bf,St}} \left(\frac{\mu_{nf}}{\mu_{bf}} \right)^2 \left(\frac{d_{nf}}{d_{bf}} \right)^{-3} \left(\frac{\rho_{nf}}{\rho_{bf}} \right)^{-1} \quad (17)$$

The friction factor of nanofluid in helical coil $f_{nf,Hc}$ was calculated using White correlation (Welti-Chanes et al., 2003) while the friction factor of nanofluid in the straight tube was taken as equal to that of the base fluid in straight tube at the same Reynolds number (Li and Xuan, 2002). Thus:

$$\frac{f_{nf,Hc}}{f_{bf,St}} = \frac{f_{nf,Hc}}{f_{nf,St}} = \left(1 - \left(1 - \left(11.6/Dn_{nf} \right)^{0.45} \right)^{2.2} \right)^{-1} \quad (18)$$

Fig. 12 shows that the pressure drop ratio (also known as pressure drop penalty factor, PF) increases with increasing Reynolds number at all concentrations used with close agreement between CFD predictions and those of equation (17). The pressure drop in helical coils using Al_2O_3 for volume fraction larger than 2% exceeds 5 times that of water in straight tubes.

Conclusions

Different heat transfer enhancement strategies in the laminar flow regime have been investigated numerically including nanofluids in straight tubes, base fluids in helical coils and nanofluids in helical coils. CFD results were validated against published experimental results and correlations. The helical coil effect enhances the heat transfer of water by up to 3.25 times compared to straight tubes which is higher than that achieved by using nanofluids in straight tubes (up to 1.55).

Additional enhancement can be achieved by adding nanoparticles where an enhancement ratio of up to 4.5 times that of base fluid (water) in straight tubes was achieved by adding Al_2O_3 nanoparticles to water in helical coils. Such enhancement is very promising for the development of nanofluids.

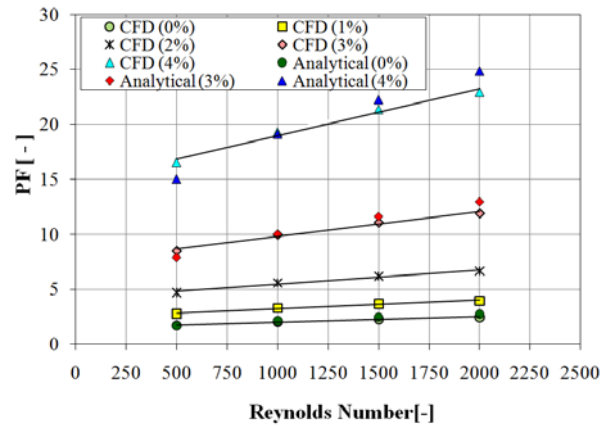For higher nanofluid concentrations, higher pressure losses have been predicted.

Fig. 12 Pressure drop penalty factor (PF) in helical coils.

Nomenculature

C   Specific heat, J/kg.K
d_{coil} Helical coil diameter, m
d_i Tube diameter, m
Dn   Dean Number
k   Thermal conductivity, W/m.K
Nu   Nusselt Number
Pr   Prandtl Number
q   Heat flux, W/m^2
Re   Reynolds number
T   Temperature, K
x   Local distance from tube entrance, m
V   Velocity, m/s
ϕ Volume fraction, -

μ Fluid viscosity, Pa.s
ρ Fluid density, kg/m^3
α Heat transfer coefficient, W/m^2K
ΔP Pressure drop, Pa

References

Akhavan-Behbadi, M.A., Hashemi, S.M., 2010. Pressure drop characteristics of nanofluid flow in horizontal coiled tube under constant heat flux. , In: Biennial Conference in Engineering Systems Design and Analysis, ASME, Turkey.

Bergles, A. E, 2002. ExHFT for fourth generation heat transfer technology. Exp. Therm Fluid Sci. 26, 335–344.

Cheng, L., 2009. Nanofluid heat transfer technologies. Recent Patents on Engineering 3, 1-7.

Elsayed, A., Al-dadah, R., Mahmoud, S., Soo, L., 2010. Experimental investigation of heat transfer in flow boiling inside a helically coiled small diameter tube. In: Proceedings of Microfluidics 2010 conference, France.

Engineering equation solver (EES) software.www.fchart.com

Heris, S.Z., Etamad, S. Gh., Esfahani, M. N, 2006. Heat transfer enhancement of nanofluid laminar flow. In: 14th Annual International Mechanical Engineering Conference, Isfahan, Iran.

Kalb, C. E., Seader, J. D., 1972. Heat and mass transfer phenomena for viscous flow in curved circular tubes. Int. J. Heat Mass Transfer 15, 801-817.

Kumar,V., Saini, S., Sharma, M., Nigam, K.D.P. 2006. Pressure drop and heat transfer study in tube-in-tube helical heat exchanger. Chem. Eng. Sci. 61, 4403-4416.

Murshed, S. M., Leong, K.C., Yang,C., Nam-Trung, N., 2007. Convective heat transfer of nanofluids in minichannel under laminar flow conditions. In: Proceedings of the International Conference on Mechanical Engineering, ICME2007, Bangladesh.

Li, Q., Xuan, Y., 2002. Convective heat transfer and flow characteristics of Cu-water nanofluid. International Journal of Nanotechnology and Applications, Science in China 45(4)-Series E, 408-416.

Rea, U., McKrell,T., Hu,L., Buongiorno,J., 2009. Laminar convective heat transfer and viscous pressure loss of alumina-water and zirconia-water nanofluid. Int. J. Heat Mass Transfer 52(7-8), 2042-2048.

Rohsenow, W. M., Hartnett, J. R., Cho, Y. I. ,1998. Handbook of heat transfer. (3rd ed.). McGraw-Hill, (Chapter 5).

Saripella, S.K., Routbort, J. L., Yu, W., France, D.M., Rizwan-Uddin, 2007. Effects of nanofluid coolant in a class 8 truck engine. Retrieved April 5, 2011 from http://papers.sae.org/2007-01-2141

Shao, L., Han, J.t., Su, G.p., Pan, J.h., 2007. Condensation heat transfer of R-134A in horizontal straight and helically coiled tube-in-tube heat exchangers.J. Hydrodyn. Ser. B 19(6), 677-682.

Sundar, L.S., Ramanathan, S., Sharma K.V., Sekhar Babu, P., 2007. Temperature Dependent Flow Charecteristics of Al_2o_3 Nanofluid. International Journal of Nanotechnology and Applications 1(2), 35-44.

Wallace, K. G., 2010. Research in heat transfer with nanofluids. M.Sc. in Technology Purdue University Calumet School of Technology.

Welti-Chanes,J. , Vélez-Ruiz,J. , Barbosa-Cánovas,J.V., 2003. Transport Phenomena in Food Processing. CRC Press LLC, (Chapter25).

Wongwises, S., Polsongkram, M., 2006a. Evaporation heat transfer and pressure drop of HFC-134a in a helically coiled concentric tube-in-tube heat exchanger. Int. J. Heat Mass Transfer 49(3-4), 658-670.

Wongwises, S., Polsongkram, M., 2006b. Condensation heat transfer and pressure drop of HFC-134a in a helically coiled concentric tube-in-tube heat exchanger. Int. J. Heat Mass Transfer 49 (23-24), 4386–4398.